Beryllium Abundances of Solar-Analog Stars[*][†]

Yoichi TAKEDA,[1] Akito TAJITSU,[2] Satoshi HONDA,[3] Satoshi KAWANOMOTO,[1]
Hiroyasu ANDO,[1] and Takashi SAKURAI[1]

[1]*National Astronomical Observatory of Japan, 2-21-1 Osawa, Mitaka, Tokyo 181-8588*

takeda.yoichi@nao.ac.jp, kawanomoto.satoshi@nao.ac.jp, ando.hys@nao.ac.jp, sakurai@solar.mtk.nao.ac.jp

[2]*Subaru Telescope, 650 North A'ohoku Place, Hilo, Hawaii 96720, USA*

tajitsu@subaru.naoj.org

[3]*Kwasan Observatory, Graduate School of Science, Kyoto University, 17 Ohmine-cho, Kita Kazan, Yamashina-ku, Kyoto 607-8471*

honda@kwasan.kyoto-u.ac.jp

Abstract

An extensive Be abundance analysis was conducted for 118 solar analogs (along with 87 FGK standard stars) by applying the spectrum synthesis technique to the near-UV region comprising the Be II line at 3131.066 Å, in an attempt to investigate whether Be suffers any depletion, such as in the case of Li showing a large diversity. We found that, while most of these Sun-like stars are superficially similar in terms of their A(Be) (Be abundances) around the solar value within $\sim \pm 0.2$ dex, 4 out of 118 samples turned out to be strikingly Be-deficient (by more than ~ 2 dex), and these 4 stars belong to the group of lowest $v_e \sin i$ (projected rotation velocity). Moreover, even for the other majority showing an apparent similarity in Be, we can recognize a tendency that A(Be) gradually increases with an increase in $v_e \sin i$. These observational facts suggest that any solar analog star (including the Sun) generally suffers some kind of Be depletion during their lives, where the rotational velocity (or the angular momentum) plays an important role in the sense that the depletion tends to be enhanced by slower rotation. Hence, our findings require that the occasionally stated view "G-type dwarfs with $T_{\rm eff} \lesssim 6000$ K are essentially homogeneous in Be with their original composition retained" should be revised. Also, our analysis indicates that the difference of ~ 0.2 dex in A(Be) between the solar photosphere and the meteorite really exists, implying that the "UV missing opacity" is irrelevant at least for this Be II line.

Key words: stars: abundances — stars: atmospheres — stars: late-type — stars: rotation — Sun: abundances

1. Introduction

This paper is the third of the series, resulting from our recent research project on a large homogeneous sample of solar analog stars, which aims to clarify the behavior of their Li abundances in connection with the stellar properties, such as rotation, stellar activity, and age. We now here focus on Be, another light element similar to Li.

1.1. Li in Solar-Analog Stars

As Li nuclei are burned and destroyed when they are conveyed into the hot stellar interior ($T \gtrsim 2.5 \times 10^6$ K), we can gain from its surface composition valuable information regarding the past history and the physical mechanism of stellar envelope mixing. Especially, the behavior of A(Li)[1] (Li abundances) in Sun-like stars is of particular interest, since it poses intriguing puzzles:

— (1) Why A(Li)'s show a remarkably large diversity (~ 2 dex), even for stars with very similar parameters (e.g., Takeda & Kawanomoto 2005)?

— (2) Why planet-host stars show markedly lower A(Li) than non-planet-host stars around the solar $T_{\rm eff}$ region (e.g., Israelian et al. 2009)?[2]

Since such characteristic trends are difficult to explain by the naive classical picture of surface Li being determined by age (duration time of gradual Li depletion by way of convective mixing) and $T_{\rm eff}$ (affecting the depth of convection zone), it has been the central task to find the key parameter(s) responsible for these observed facts.

In an attempt toward clarifying this issue, Takeda et al. (2007; hereinafter referred to as Paper I) conducted an extensive study on the connection of Li abundances and stellar parameters for 118 solar analogs, and found that A(Li) is found to closely correlated with the line-width (combination of rotation and macroturbulence), from which they suspected that rotation may be the key factor. Successively, Takeda et al. (2010; hereinafter referred to as Paper II) studied the residual flux at the core of the strong Ca II 8542 line [r_0(8542); a good indicator of stellar activity, considered to be rotation-dependent because of its dynamo origin] for these 118 stars, and confirmed that r_0(8542) shows a positive connection with

---

[*] Based on data collected at Subaru Telescope, which is operated by the National Astronomical Observatory of Japan.

[†] The large data are separately given in the electronic form (tables E1, E2, and E3), which will be available at the E-PASJ web site ⟨http://pasj.asj.or.jp/v63n3/630330/⟩.

[1] Throughout this study, A(X) means the logarithmic (number) abundance of any element (X) in the usual normalization of A(H) = 12, whereas we express the logarithmic differential abundance of X relative to the Sun by [X/H] [$\equiv A_{\rm star}$(X) $- A_\odot$(X)].

[2] Critical arguments against the existence of such a characteristic behavior of Li specific to planet-host stars also exist (e.g., Baumann et al. 2010).
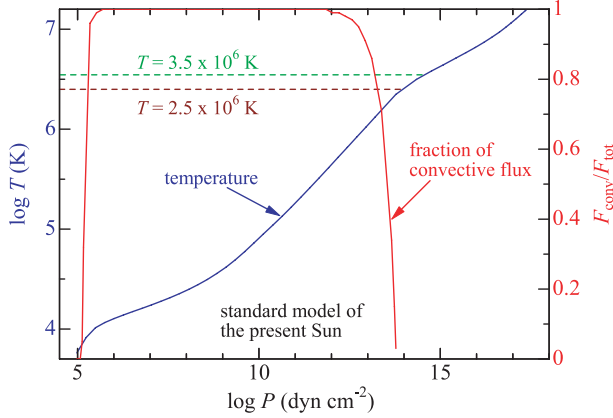
Fig. 1. Temperature (T) and fraction of the convective flux ($F_{\mathrm{conv}}/F_{\mathrm{total}}$) for the standard solar model (Stix 2002), plotted against pressure (P). The critical temperatures of Li-burning ($T \sim 2.5 \times 10^6$ K) and Be-burning ($T \sim 3.5 \times 10^6$ K) are indicated by horizontal dashed lines.

the line width as well as A(Li). Thus, there is no doubt that the stellar angular momentum plays the decisive role in controlling the surface Li abundances of Sun-like stars, in the sense that Li tends to be more depleted for slowly rotating stars. [See, e.g., Pinsonneault 2010 for a review regarding the impact of rotatinal mixing on the surface Li abundance of late-type stars.]

1.2. Be: Another Probe

Thus, the next task should be to find a theoretical explanation that reasonably accounts for the observational fact. Interestingly, Bouvier (2008) recently proposed a promising mechanism that slow rotation can produce efficient mixing as well as Li depletion. He showed in his theoretical simulation that slow rotators develop a high degree of differential rotation between the radiative core and the convective envelope, which eventually promotes Li depletion by enhanced mixing, while fast rotators evolve with little such core–envelope decoupling. If such a picture is correct, the key to understanding the mixing mechanism lies in "the bottom of the convection zone," where shear instability induced by differential rotation takes place in slow rotators.

We should point out that the best way to probe the condition of this deep layer is to study the abundance of Be (destroyed at temperature of $T \gtrsim 3.5 \times 10^6$ K; i.e., somewhat higher than the Li-burning temperature) along with that of Li. According to figure 1, where the T–P and $F_{\mathrm{conv}}/F_{\mathrm{tot}}$–$P$ relations of the standard solar model (Stix 2002) are depicted, the critical temperatures of Li as well as Be burning just lie near to the base of the convection zone. Therefore, we should be able to extract useful information about this critical layer by examining/comparing the abundances of these two elements for a large sample of solar analogs having a wide variety of rotational velocities, which might serve as a good touchstone for a theory of the mixing mechanism.

1.3. Controversy on Be in Solar-Type Stars

Unfortunately, no consensus has yet been accomplished concerning the behavior of Be in solar-analog stars.

— Santos et al. (2004a) suggested from their extensive Be abundance analysis of FGK stars (6300 K $\gtrsim T_{\mathrm{eff}} \gtrsim$ 4800 K) that a significant Be depletion in a narrow T_{eff} range (similar to the Li gap for F-type stars) may exist in solar-temperature stars.

— Meanwhile, Randich (2010) argued that Be abundances are generally uniform (i.e., with almost no sign of depletion) in G-type dwarfs with $T_{\mathrm{eff}} \lesssim 6000$ K, regardless of the large spread of Li abundances (in contrast to F-type stars with $T_{\mathrm{eff}} \gtrsim 6000$ K showing appreciable Be deficiencies in accordance with Li), which means that Li and Be do not have any correlation in Sun-like stars.

— Takeda and Tajitsu (2009) determined the Li and Be abundances for three solar twins (HIP 56948, HIP 79672, and HIP 100963) along with the Sun, and concluded that all three have essentially the same A(Be) with the solar value, in spite of the marked difference in A(Li).

— Stephens et al. (1997) reported, in their extensive Be abundance investigation for $\sim$ 60 Li-deficient stars, that some early-G stars at $T_{\mathrm{eff}} \lesssim 6000$ K exhibit moderate Be deficiencies by a factor of $\sim$2–4 (apart from the considerable Be depletion for F stars at 6000 K $\lesssim T_{\mathrm{eff}} \lesssim 6800$ K).

— Boesgaard and Hollek's (2009) Be abundance study for 50 "one solar mass" stars (6500 K $\gtrsim T_{\mathrm{eff}} \gtrsim$ 5600 K) revealed several 3–4 very Be-depleted stars despite that most stars are quite homogeneous in [Be/Fe]; however, since these outliers are either subgiants or $T_{\mathrm{eff}} > 6000$ K dwarfs, it still remains an open question whether Be depletion occurs in solar analogs.

Hence, it is still unsettled in which condition Be is depleted (or not depleted) along with Li in G-dwarfs similar to the Sun. While clarifying this issue is requisite for understanding the mechanism of how depletion takes place (e.g., the penetration depth of mixing at the bottom of the convection zone), the available observational data do not seem to be sufficient, because a systematic Be abundance study specifically directed to a large homogeneous sample of "solar analog stars" has never been carried out to our knowledge.

1.4. Purpose of This Study

Given this situation, we decided to determine the Be abundances of 118 solar analogs, for which Li abundances and various stellar parameters have already been well established in Papers I and II, by using the Be II doublet lines at 3130–3131 Å based on the high-dispersion near-UV spectra obtained by Subaru/HDS (just suitable because of its sufficiently high efficiency down to $\lambda \sim 3000$ Å thanks to the near-UV-sensitive CCD as well as the high-transparency at Mauna Kea summit), in order to investigate whether any meaningful correlation exists between A(Be) and A(Li), and whether they show any dependence upon the stellar physical parameters (e.g., stellar rotation, T_{eff}, age, activity index, etc.). This is the aim of the present investigation.

The remainder of this paper is organized as follows. After describing the targets and the observational data (section 2), we explain the details of abundance determinations in section 3, followed by section 4 where the results of Be abundances are examined and discussed, first for FGK standard stars and then for solar analog stars. The conclusion is summarized in section 5. In addition, an appendix is prepared where

the non-LTE effect on Be abundance determination from the Be II 3131 line is mentioned.

2. Observational Data

2.1. Target Stars

The main targets in this investigation are the 118 solar analogs studied in detail in Papers I and II, for which the atmospheric parameters [the effective temperature ($T_{\rm eff}$), surface gravity ($\log g$), microturbulent velocity dispersion ($v_{\rm t}$), and metallicity (represented by Fe abundance relative to the Sun; [Fe/H])], the Li abundance [A(Li)], and the stellar parameters [the luminosity (L), mass (M), and age (age)] were already established (cf. sections 3 and 4 in Paper I). Besides, the residual flux at the line center of the Ca II 8542 [r_0(8542); good indicator of stellar activity] and the projected rotational velocity ($v_{\rm e}\sin i$) were also evaluated in Paper II (cf. sections 2 and 3 therein).

In addition, we also included 87 FGK stars (mostly dwarfs but including several subgiants) selected from 160 standard stars, which were studied in detail by Takeda et al. (2005; atmospheric parameters), Takeda and Kawanomoto (2005; Li abundances), and Takeda (2007; elemental abundances and stellar parameters such as age). These stars (ranging in $7000\,{\rm K} \gtrsim T_{\rm eff} \gtrsim 5000\,{\rm K}$) were added mainly for the purpose of checking the behavior of Be in the wider range of $T_{\rm eff}$ by comparing it with published results.

Three kinds of representative parameter correlations ($\log g$ vs. $T_{\rm eff}$, $\log L$ vs. $\log T_{\rm eff}$, and [Fe/H] vs. $\log age$) for the program stars are depicted in figure 2, where we can recognize a remarkable similarity of the parameters as well as a rather tight age–metallicity relation for the 118 solar analogs (black filled circles). The fundamental data (magnitudes, colors, stellar parameters, etc.) for all of our target stars are summarized in electronic table E1.

2.2. Observations

Observations of 205 targets (118 solar analogs and 87 standard stars) and Vesta (substitute for the Sun) were carried out on 4 nights (Hawaii Standard Time) of 2009 August 6, 2009 November 27, 2010 February 4, and 2010 May 24 with the High Dispersion Spectrograph (HDS: Noguchi et al. 2002) placed at the Nasmyth platform of the 8.2-m Subaru Telescope, by which high-dispersion spectra covering ~ 3000–$4600\,$Å could be obtained with two CCDs of $2\,{\rm K} \times 4\,{\rm K}$ pixels in the standard Ub setting with the blue cross disperser. The spectrum resolving power was $R \simeq 60000$ with the slit width set at $0.''6$ (300 μm) and a binning of 2×2 pixels. The typical integrated exposure times were ~ 10–20 min for solar analogs (typically $V \sim 8$) and $\sim$ several min for standard stars (typically $V \sim 5$). The basic data of these spectra (observing date, exposure time, S/N ratio, etc.) are given in electronic table E1.

2.3. Data Reduction

Reduction of the spectra (bias subtraction, flat-fielding, scattered-light subtraction, spectrum extraction, wavelength calibration, co-adding of frames to improve S/N, continuum normalization) was performed by using the "echelle" package
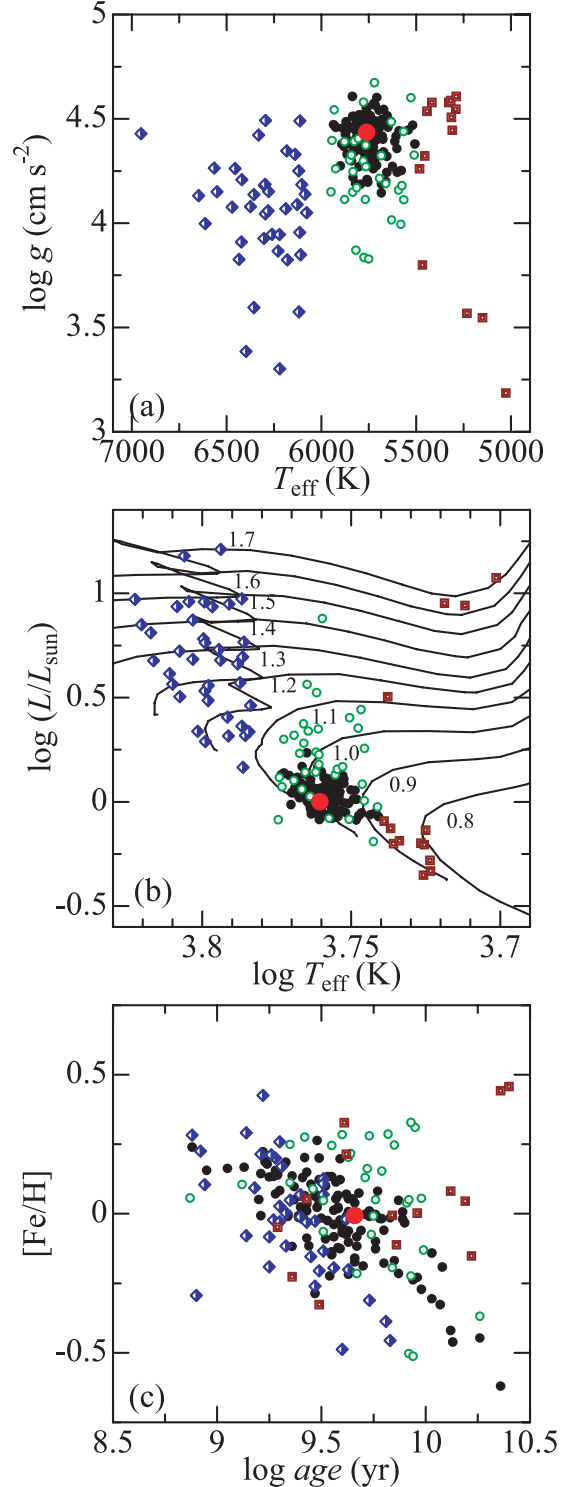

Fig. 2. Correlations of representative stellar parameters for the program stars: (a) surface gravity vs. effective temperature, (b) luminosity vs. effective temperature [Girardi et al.'s (2000) theoretical evolutionary tracks for the solar metallicity stars of $0.8\,M_\odot$ to $1.7\,M_\odot$ are also shown], and (c) age vs. metallicity. Filled (black) circles $\cdots$ 118 solar analogs, half-filled (blue) diamonds $\cdots$ 39 standard stars of F-type ($7000\,{\rm K} > T_{\rm eff} > 6000\,{\rm K}$); open (green) circles $\cdots$ 34 standard stars of early G type ($6000\,{\rm K} > T_{\rm eff} > 5500\,{\rm K}$); outlined (brown) squares $\cdots$ 14 standard stars of late G- or early K-type ($5500\,{\rm K} > T_{\rm eff} > 5000\,{\rm K}$). The large (red) circle indicates the Sun.

of the software IRAF[3] in a standard manner. Typical S/N ratios of ~ 100 were attained at the position of the Be II 3130–3131 doublet lines in the finally resulting spectra for most of the targets.

3. Be Abundance Determination

3.1. Basic Strategy

Since Be II 3130–3131 doublet lines, on which we rely for Be abundance determinations, are located in the UV region heavily crowded with a number of spectral lines, applying the spectrum synthesis technique is requisite. Regarding the data of atomic/molecular lines, we exclusively adopted Primas et al.'s (1997) line list. Figure 3a shows a comparison of theoretical and observed (flux) spectra of the Sun in the 3128–3133 Å region, while the used line data are presented in table 1 along with information about each line's strength. [Note that, in figures 3a and b, the calculation was carried out with the standard solar abundances and no attempt was made to fit the theoretical spectrum with the observed one by adjusting the abundances.]

Inspecting figure 3a and table 1, we decided to use only the Be II 3131.066 line (weaker one of the doublet), since the stronger Be II 3130.421 line is unsuitable because of being heavily blended with nearby V II or OH lines. Here, the critical point we should attend is that Be II 3131.066 is blended with Fe I 3131.043;[4] the contribution of the latter must therefore be removed for a reliable Be abundance determination.

Therefore, we focused on the 3130.65–3131.35 Å region (cf. figure 3b) comprising three conspicuous features: the left one is due to blends of Nb II 3130.780 and Ti II 3130.810 lines, the middle one is due to Fe I 3131.043 and Be II 3131.066, and the right one is primarily due to Fe I 3131.235 line (actually a composite of Cr I, Fe I, and Tm II lines). We may then hope that the Be abundance can be reasonably established, since the contribution of Fe I 3131.043 may be controlled by simultaneously considering the Fe I 3131.235 line, while the Nb II+Ti II feature contains information to regulate the line broadening. Accordingly, our abundance determination is based on matching between theoretical and observed spectra in this 3130.65–3131.35 Å region by adjusting the abundances of these 4 elements (Be, Cr, Fe, Nb) along with the line-broadening function.
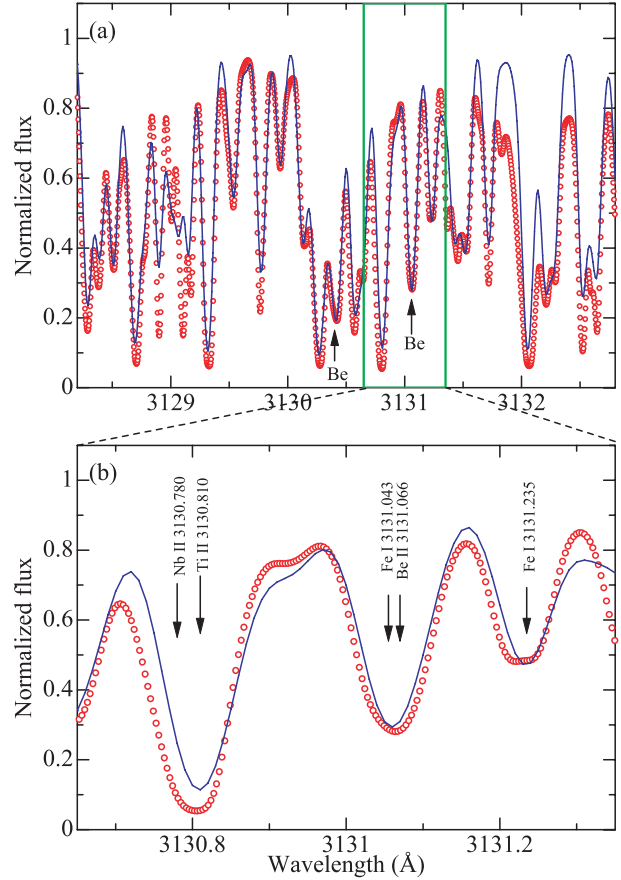

Fig. 3. Theoretically synthesized spectrum for the Sun (blue solid line), where the gf values in table 1 were used along with Anders and Grevesse's (1989) standard solar photospheric abundances (except for Fe, for which we adopted 7.50), compared with Kurucz et al.'s (1984) solar flux spectrum (red open circles). (a) 3128.2–3132.8 Å region; (b) 3130.65–3131.35 Å region [magnification of (a)].

3.2. Spectrum Fitting Analysis

Practically, we used a stellar spectrum analysis tool, "MPFIT", which was developed based on Kurucz's (1993) ATLAS9/WIDTH9 program and has a function of establishing the spectrum-related parameters (elemental abundances, macrobroadening parameters, radial velocity, etc.) by automatically searching for the best-fit solutions without any necessity of precisely placing the continuum level (Takeda 1995).

We interpolated Kurucz's (1993) grid of ATLAS9 model atmospheres in terms of $T_{\rm eff}$, $\log g$, and [Fe/H] to generate the atmospheric model for each star. The assumption of LTE (local thermodynamical equilibrium) was adopted throughout this study, since the non-LTE effect on Be abundance determination from the Be II resonance doublet at 3030–3031 Å is insignificant (almost negligible especially for solar-analog stars), as separately discussed in the Appendix. Besides, the effect of atmospheric inhomogeneity (3D effect) is also unimportant for the deep-forming Be II lines according to Asplund (2005), by which the use of the classical treatment is justified.

Thus, given the atmospheric model, we determined for each

---

[3] IRAF is distributed by the National Optical Astronomy Observatories, which is operated by the Association of Universities for Research in Astronomy, Inc. under a cooperative agreement with the National Science Foundation.

[4] Although this line has not been confirmed from atomic physics, but just empirically assumed by Primas et al. (1997) in order to reproduce the real spectrum of a Be-depleted star, we regard that this identification is surely reasonable (cf. subsection 3.3). We should note, however, that other possibilities of line blending with the Be II 3131.066 line have also been considered in previous studies. For example, García López et al. (1995b) included Mn I 3131.037 line ($\chi_{\rm low} = 3.77$ eV) along with its appropriately adjusted $\log gf$, instead of the Fe I 3131.043 we adopted. Further, King et al. (1997) carefully examined the blending effect of other lines such as those of Mn II or Ti II or CH (in addition to this Mn I 3131.037 line) with an aim to reproduce the blue wing of the Be II 3131.066 line.

Table 1. Adopted data of atomic and molecular lines.

Species	λ (Å)	χ (eV)	log gf	η₀	Species	λ (Å)	χ (eV)	log gf	η₀	Species	λ (Å)	χ (eV)	log gf	η₀
OH	3128.060	0.54	−2.73	1.17	Cr I	3129.774	2.71	−2.46	0.04	Tm II	3131.257	0.00	+0.28	1.36
OH	3128.101	0.21	−3.18	0.79	Fe I	3129.802	2.88	−2.80	1.66	OH	3131.329	1.94	−1.80	0.59
OH	3128.237	0.44	−3.32	0.36	Cr I	3129.858	2.97	−2.27	0.04	OH	3131.384	1.68	−3.22	0.04
Sc II	3128.269	3.46	−0.17	0.25	Y II	3129.935	3.42	+0.98	1.04	OH	3131.393	1.68	−3.29	0.03
OH	3128.286	0.21	−2.29	6.24	OH	3129.938	1.61	−1.84	1.05	Fe II	3131.395	3.81	−3.46	0.89
OH	3128.290	0.44	−3.14	0.55	Gd II	3129.968	1.17	−0.20	0.11	OH	3131.423	0.96	−2.16	1.84
V II	3128.305	2.38	−0.87	1.83	Zr I	3130.056	0.52	−0.95	0.02	Fe I	3131.455	2.47	−3.60	0.60
OH	3128.356	1.72	−2.61	0.14	OH	3130.125	0.84	−2.15	2.40	Fe I	3131.460	2.47	−4.53	0.07
OH	3128.376	1.72	−3.48	0.02	Ti I	3130.158	1.98	−0.46	0.64	OH	3131.501	0.50	−2.73	1.25
CH	3128.393	0.56	−1.34	1.55	Fe I	3130.205	3.33	−2.60	1.05	Ni I	3131.525	3.19	−2.90	0.09
CH	3128.393	0.56	−1.30	1.69	V II	3130.258	0.35	−0.74	145.76	Cr II	3131.533	4.17	−1.51	2.95
Dy II	3128.406	1.31	+0.35	0.56	OH	3130.280	0.25	−1.97	11.80	Cr II	3131.548	4.18	−1.46	3.25
Ti II	3128.490	3.90	−0.02	4.88	Ce II	3130.340	0.53	−0.15	0.49	OH	3131.686	1.74	−2.51	0.17
OH	3128.518	0.79	−2.49	1.23	CH	3130.370	0.03	−1.96	1.07	Ni I	3131.702	3.31	−1.61	1.42
OH	3128.525	0.10	−3.30	0.75	Ti I	3130.376	1.43	−1.56	0.15	OH	3131.710	1.74	−3.50	0.02
Cr II	3128.545	4.76	−2.07	0.25	OH	3130.407	1.76	−3.49	0.02	Fe II	3131.724	4.08	−2.10	11.85
Gd II	3128.569	1.13	−0.10	0.15	Be II	3130.421	0.00	−0.17	9.97	OH	3131.755	0.96	−3.26	0.15
Ti I	3128.627	2.10	−0.49	0.47	OH	3130.432	1.76	−2.37	0.23	Co I	3131.826	1.74	−2.59	0.10
Mn II	3128.640	6.67	−1.15	0.03	OH	3130.473	1.61	−3.22	0.04	Cr II	3132.053	2.49	−0.32	1335.65
Cr II	3128.692	2.43	−0.72	589.75	Fe I	3130.476	3.58	−2.96	0.28	Zr I	3132.063	0.54	+0.02	0.22
Cu I	3128.692	4.97	−0.71	0.05	Mn II	3130.551	6.49	−1.15	0.04	OH	3132.186	0.90	−2.32	1.46
V II	3128.694	2.37	−0.67	2.97	Cr II	3130.568	5.33	−2.46	0.03	Co I	3132.212	0.10	−2.52	3.09
Ni I	3128.728	1.95	−4.29	0.04	OH	3130.570	0.68	−1.78	7.81	CH	3132.281	0.49	−1.38	1.61
Y II	3128.737	3.38	+0.81	0.76	Cr I	3130.585	3.56	−1.97	0.02	CH	3132.281	0.49	−1.33	1.82
OH	3128.783	0.90	−2.29	1.55	Mn I	3130.637	4.27	−1.01	0.11	Mn I	3132.289	4.33	−0.50	0.32
Fe I	3128.897	1.56	−3.05	13.14	CH	3130.648	0.03	−1.55	2.72	Mn I	3132.405	3.38	−2.09	0.06
OH	3128.975	1.94	−1.77	0.63	Nb II	3130.780	0.44	+0.41	5.85	Er II	3132.517	1.40	+0.51	0.63
Co I	3129.006	0.51	−2.93	0.53	Ti II	3130.810	0.01	−1.53	370.74	Fe I	3132.519	3.21	−1.10	42.62
Fe II	3129.009	3.97	−2.90	2.39	Gd II	3130.813	1.16	−0.08	0.15	OH	3132.584	1.61	−2.00	0.72
Ti I	3129.070	2.12	+0.49	4.31	Ce II	3130.871	1.09	+0.48	0.69	Ce II	3132.592	0.30	−0.54	0.32
OH	3129.094	0.90	−3.24	0.17	CH	3130.928	0.00	−3.14	0.07	Mo I	3132.595	0.00	−0.13	0.82
Zr II	3129.153	0.53	−0.12	20.87	OH	3130.928	1.91	−2.52	0.12	V II	3132.596	2.90	−1.07	0.41
Fe I	3129.182	2.45	−4.46	0.09	OH	3130.933	0.68	−3.13	0.34	Fe I	3132.649	3.24	−1.60	12.77
Cr I	3129.210	3.56	−1.11	0.17	Mn II	3131.015	6.11	−1.22	0.07	Ti I	3132.710	2.00	−0.77	0.30
Ni I	3129.300	0.28	−2.75	44.23	Mn I	3131.037	3.77	−1.73	0.06	Mn I	3132.789	4.27	−0.50	0.36
Fe I	3129.334	1.48	−2.49	55.00	Fe I	3131.043	2.85	−2.52	3.34	V II	3132.810	2.51	−1.53	0.31
Co I	3129.482	1.88	−2.02	0.28	Be II	3131.066	0.00	−0.47	5.00	Cr I	3132.822	3.12	−0.19	3.42
OH	3129.539	0.52	−2.62	1.57	Th II	3131.070	0.00	−1.56	0.01	OH	3132.845	1.95	−2.46	0.13
Ti I	3129.636	1.44	−1.45	0.19	Zr I	3131.109	0.52	−0.40	0.09	Ni II	3132.865	2.87	−3.65	0.79
Nb II	3129.652	1.32	−0.94	0.04	Os I	3131.116	1.84	+0.05	0.10	OH	3132.866	0.69	−3.24	0.27
Mn I	3129.667	3.77	−1.51	0.10	Cr I	3131.212	3.11	−0.66	1.18					
Zr II	3129.764	0.04	−0.65	16.37	Fe I	3131.235	2.18	−3.30	2.14					

* Atomic and molecular line data we used for spectrum synthesis. Five kinds of data are presented for each line: (1) species designation, (2) line wavelength, (3) lower excitation potential, (4) logarithm of lower statistical weight times oscillator strength, and (5) line(center)-to-continuum opacity ratio at $\tau_{5000} = 0.2$ computed for the solar case (good indicator of the observed line-strength). The data of (1)–(4) are based on the line list of Primas et al. (1997; cf. table 2 therein).

star the abundances of four elements [A(Be), A(Ti), A(Fe), and A(Nb)],[5] along with the macrobroadening parameter ($v_{\rm M}$; e-folding half-width of the Gaussian macrobroadening function, $f_{\rm M}(v) \propto \exp[(−v/v_{\rm M})^2]$) and the radial velocity shift, by applying the MPFIT program to the observed spectrum in the 3130.65–3131.35 Å region. The finally established abundances of A(Be) and A(Fe) are given in electronic table E2, and the theoretical spectra corresponding to the best-fit solutions (along with the observed spectra) are shown in figures 4 (solar analogs) and 5 (FGK standards).

3.3. EW Evaluation

Actually, there were cases where abundance solutions did not converge. When any of A(Ti), A(Fe), or A(Nb) was indeterminable, we fixed it at the metallicity-scaled solar abundance [i.e., A(Ti) $= A_{\odot}$(Ti) $+$ [Fe/H], etc.] and retried the iteration procedure for the best-fit solutions. Meanwhile, when A(Be) could not be determined (Be-depleted case of too weak Be II line), we neglected its contribution by assuming A(Be) $= −9.99$, and retried the iteration. In this case, the upper limit of the equivalent width for the Be II 3131.066 line ($EW_{\rm Be II\ 3131}^{\rm UL}$) was evaluated as $EW_{\rm Be II\ 3131}^{\rm UL} \simeq k \times$ FWHM$/(S/N)$, where k is a factor that we assumed to be 2 according to our experience, S/N is the signal-to-noise ratio ($\sim$100), and FWHM was estimated from $v_{\rm M}$ as FWHM $\simeq 2\sqrt{\ln 2}\ (\lambda v_{\rm M}/c)$ (c: velocity

---

[5] The contributions of the lines of other elements than these four (cf. table 1) were formally included by assuming the solar abundances scaled with the metallicity; i.e., A(el) $= A_{\odot}$(el) $+$ [Fe/H].
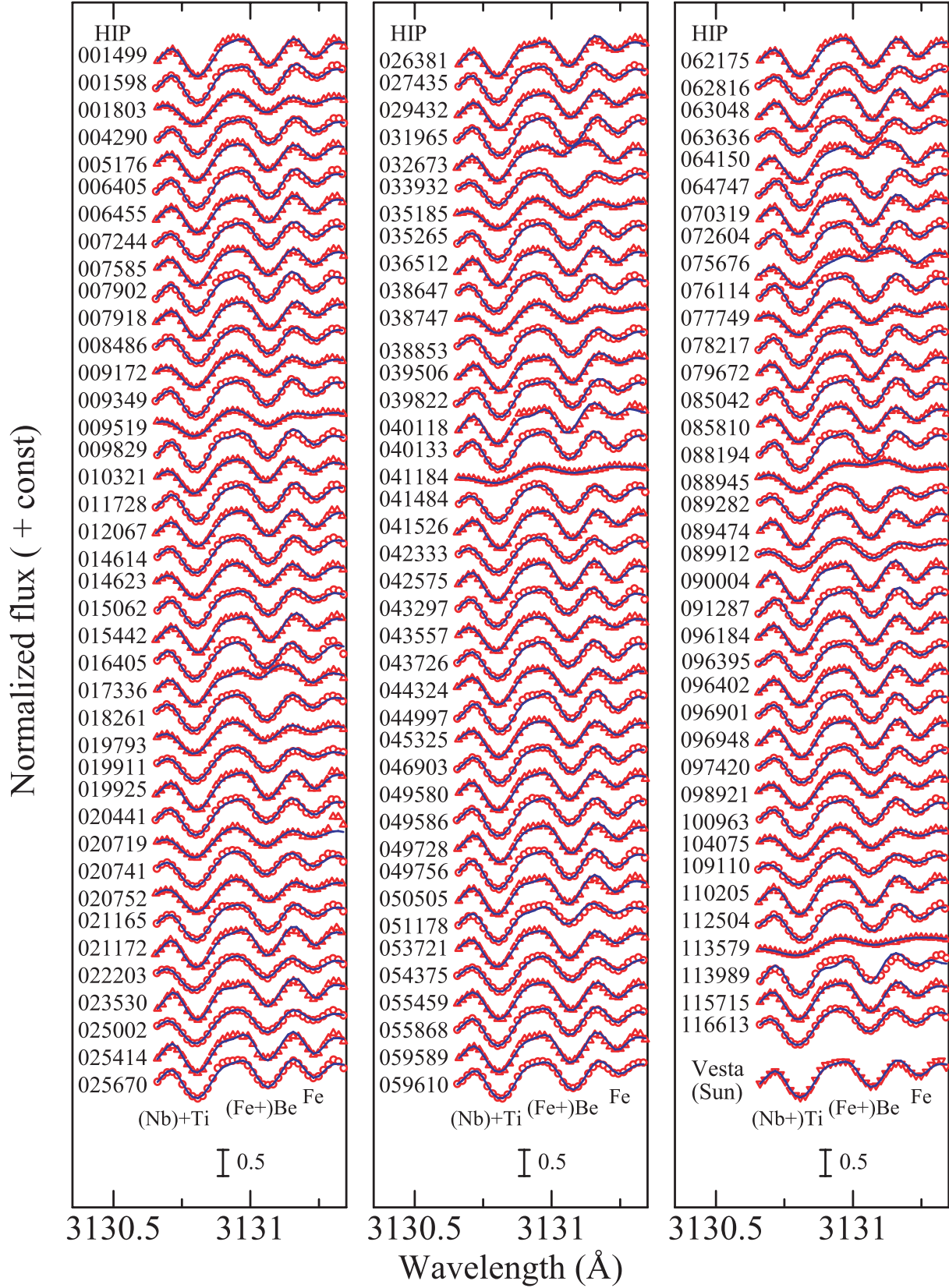
Fig. 4. Synthetic spectrum fitting in the 3130.65–3131.35 Å region for 118 solar-analog stars. The best-fit theoretical spectra are shown by solid lines, while the observed data are plotted by symbols. A vertical offset of 0.5 is applied to each relative to the adjacent ones. Each of the spectra are arranged in the increasing order of HIP number (indicated on the left to each spectrum), as in figures 6/8 in Paper I or figure 2 in Paper II, while the case of Vesta (Sun) is displayed at the bottom-right. The wavelength scale of each spectrum is adjusted to the laboratory system.
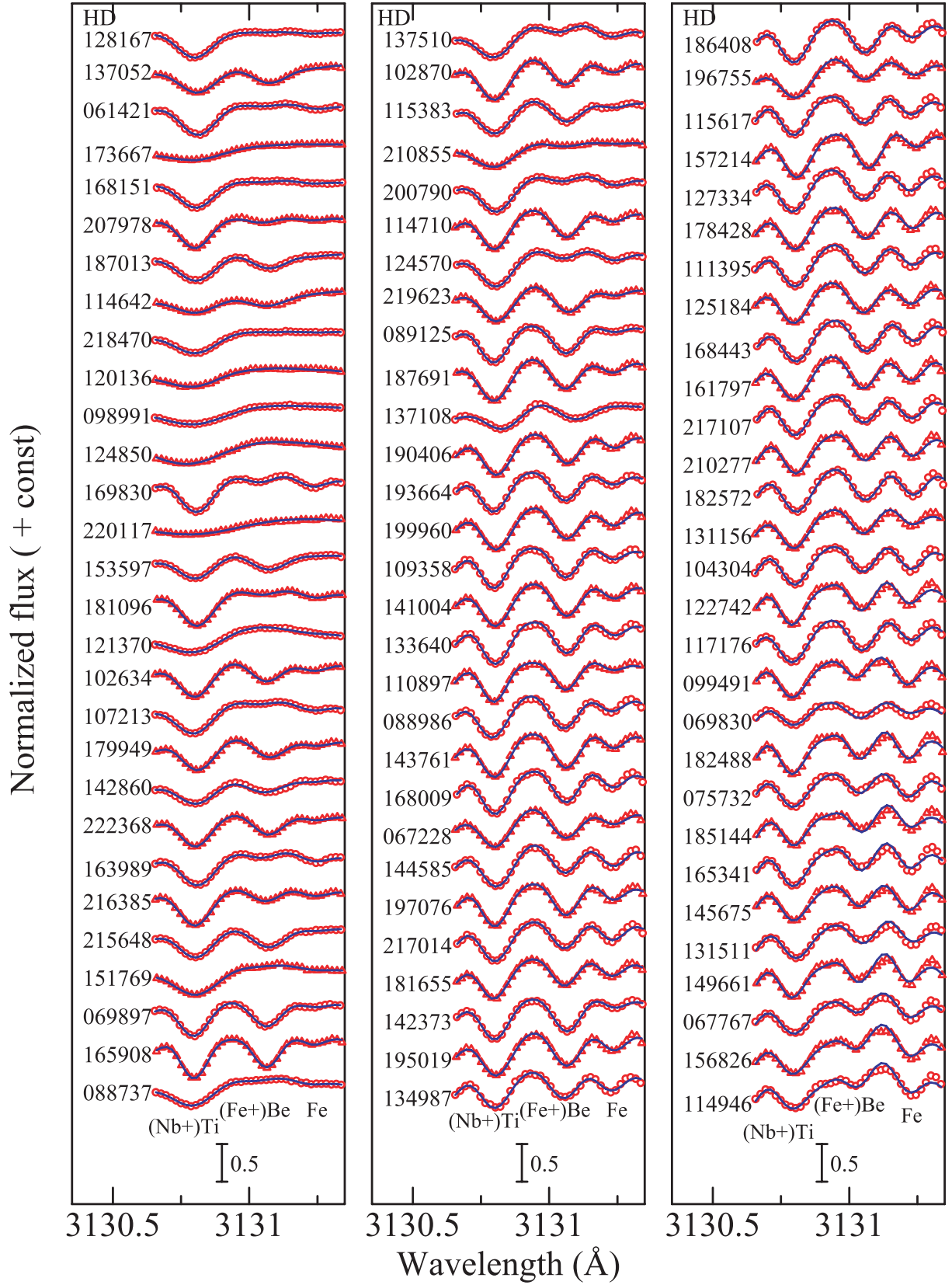
Fig. 5. Synthetic spectrum fitting in the 3130.65–3131.35 Å region for 87 standard stars of F, G, and K type. Each of the spectra are arranged in the decreasing order of T_{eff}. Indicated on the left to the spectrum is the HD number. Otherwise, the same as in figure 4.
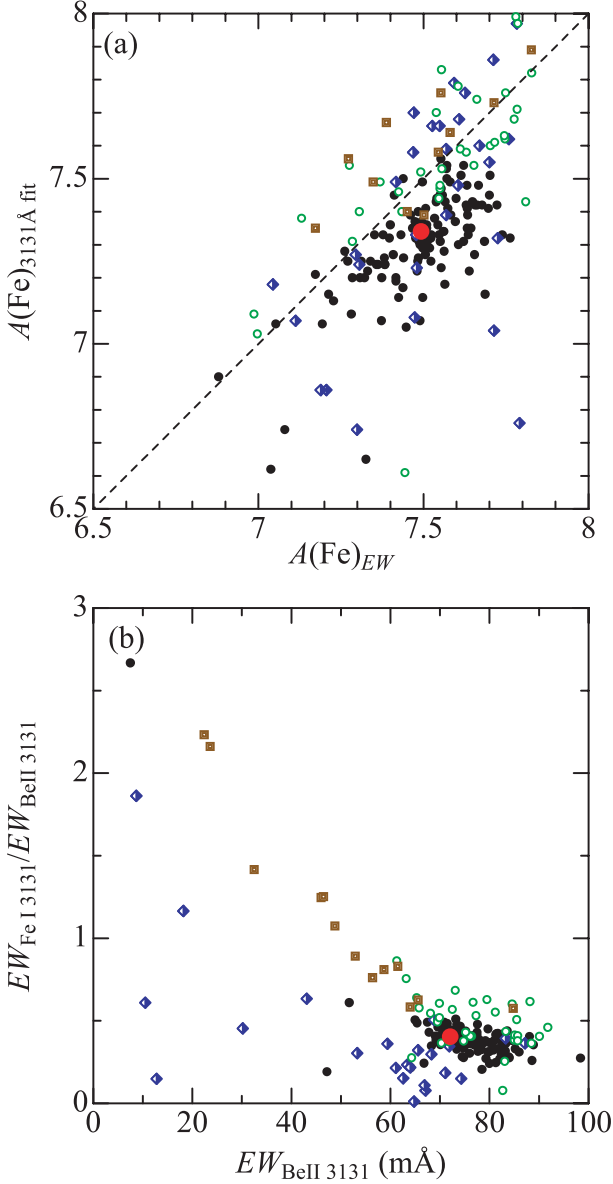
Fig. 6. (a) Correlation of the Fe abundance derived from the synthetic spectrum fitting analysis in the 3130.65–3131.35 Å region with that determined based on EWs of many Fe lines (cf. Paper I; Takeda et al. 2005). (b) Ratio of $EW_{\mathrm{Fe\,I}\ 3131.043}/EW_{\mathrm{Be\,II}\ 3131.066}$ (equivalent widths inversely computed from fitting-based abundance solutions of Fe and Be) plotted against $EW_{\mathrm{Be\,II}\ 3131.066}$. The same meanings of the symbols as in figure 2.

of light). We then derived the upper limit of $A(\mathrm{Be})$ from such obtained $EW_{\mathrm{Be\,II}\ 3131}^{\mathrm{UL}}$.

Whether the contribution of the Fe I 3131.043 line could be successfully removed can be checked by comparing $A(\mathrm{Fe})$ derived from this fitting and that already established in Paper I by using a number of Fe lines. This comparison is displayed in figure 6a, from which we can confirm that both are mostly consistent to within $\lesssim 0.2$ dex. We also computed $EW_{\mathrm{Be\,II}\ 3131}$ and $EW_{\mathrm{Fe\,I}\ 3131}$ "inversely" from $A(\mathrm{Be})$ and $A(\mathrm{Fe})$ (resulting from the spectrum synthesis analysis) along with the adopted atmospheric model/parameters, in order to examine to which

extent the Fe I line contributes to the (Fe I +) Be II feature. According to figure 6b, the strength of this Fe I line is weaker than that of the Be II line in most cases (typically $\sim 30\%$–40% for solar analogs), though the former can outweigh (or even becomes predominant over) the latter for the Be-depleted cases particularly seen for F-type stars. These two kinds of EW values are also given in electronic table E2.

3.4. Error Estimation

By using the EW values derived in the previous subsection, we tried to estimate errors involved in $A(\mathrm{Be})$ from the viewpoints of two factors: ambiguities in the adopted atmospheric parameters and uncertainties in the treatment of line blending with the Be II 3131.066 line.

The atmospheric parameters (T_{eff}, $\log g$, v_{t}) adopted in this study are the spectroscopically determined ones taken from Paper I (solar analogs) and Takeda et al. (2005) (FGK stars). These parameters were numerically derived (i.e., independently from any subjective judgement by human eye) based on the EWs measured for a number of Fe I and Fe II lines, while invoking the program TGVIT (Takeda et al. 2002, 2005), which establishes the best solutions satisfying (a) the independence of $A(\mathrm{Fe})$ upon χ_{low}, (b) the independence of $A(\mathrm{Fe})$ upon EW, and (c) matching of $\langle A(\mathrm{Fe\,I})\rangle$ and $\langle A(\mathrm{Fe\,II})\rangle$. The intrinsic ambiguities involved in these solutions may be defined as the extents of the range, within which any change in the relevant parameter does not cause any substantial influence on the judgement that these three requirements, (a)–(c) are fulfilled (see subsection 5.2 of Takeda et al. 2002 for more details of the practical numerical procedures). Such derived uncertainties in T_{eff}, $\log g$, and v_{t} (along with the parameter solutions themselves) for all of the program stars are presented in electronic table E3. As can be seen from these results, typical ambiguities[6] are on the order of $\sim \pm 20$ K in T_{eff}, $\sim \pm 0.05$ dex in $\log g$, and $\sim \pm 0.1$ km s^{-1} in v_{t} (within a factor of $\lesssim 2$; see also subsection 3.1 in Paper I and table E3 of Takeda et al. 2005). The Be abundance error corresponding to such estimated parameter uncertainties [$e(T_{\mathrm{eff}})$, $e(\log g)$, $e(v_{\mathrm{t}})$] for each star was evaluated as follows. From the equivalent width of the Be II line ($EW_{\mathrm{Be\,II}\ 3131}$) described in the previous subsection, six kinds of abundances were derived while varying each of the standard values of atmospheric parameters interchangeably by $+e(T_{\mathrm{eff}})$, $-e(T_{\mathrm{eff}})$, $+e(\log g)$, $-e(\log g)$, $+e(v_{\mathrm{t}})$, and $-e(v_{\mathrm{t}})$; and we call the differences of these perturbed abundances from the standard one as δ_{T+}, δ_{T-}, δ_{g+}, δ_{g-}, δ_{v+}, and δ_{v-}, respectively. We then computed the root-sum-square of three quantities $\delta_{Tgv} \equiv (\delta_T^2 + \delta_g^2 + \delta_v^2)^{1/2}$ as the abundance uncertainty (due to combined errors in T_{eff}, $\log g$, and v_{t}), where δ_T, δ_g, and δ_v are defined as $\delta_T \equiv (|\delta_{T+}| + |\delta_{T-}|)/2$, $\delta_g \equiv (|\delta_{g+}| + |\delta_{g-}|)/2$, and $\delta_v \equiv (|\delta_{v+}| + |\delta_{v-}|)/2$, respectively. The resulting values of δ_{T+}, δ_{T-}, δ_{g+}, δ_{g-}, δ_{v+}, δ_{v-}, and δ_{Tgv} for all the program stars are also given in electronic table E3. An inspection of these results revealed, however, that δ_{Tgv} is only a few hundredths dex (~ 0.02–0.06 dex) in most cases, which

---

6   The uncertainties quoted here are the "internal" statistical errors being valid only in the relative sense within stars whose parameters were established in the same consistent manner. We can not say here anything about systematic errors involved in the absolute parameter values (e.g., those due to imperfectness of the adopted atmospheric model, etc.).

is mainly determined by δ_g (being larger than δ_T and δ_v by a factor of ~ 3–4). This indicates that the statistical errors in the atmospheric parameters are practically insignificant for the results of Be abundances.

Next, we tried to roughly estimate how much errors in A(Be) may result from ambiguities in the contribution of the Fe I 3131.043 line. As mentioned in subsection 3.3 (figure 6a), the Fe abundances derived from the fitting analysis turned out to be more or less in accord with the [Fe/H] values resulting from EWs of a number of Fe lines as a by-product of parameter determinations (Paper I; Takeda et al. 2005). Yet, an appreciable dispersion ($\sim \pm 0.2$ dex) shown in figure 6a may be regarded as a measure of the uncertainties in the treatment of the blending effect. Accordingly, we proceeded as follows. We first derived $EW'_{\mathrm{FeI\ 3131}}$ by using the fixed Fe abundance corresponding to the [Fe/H] value (instead of the Fe abundance obtained as the fitting solution) for each star, and then computed the difference $\delta EW [\equiv EW'_{\mathrm{FeI\ 3131}} - EW_{\mathrm{FeI\ 3131}}]$. Under the assumption that the sum of $EW_{\mathrm{BeII\ 3131}} + EW_{\mathrm{FeI\ 3131}}$ remains invariable, we corrected EW for the Be II line as $EW'_{\mathrm{BeII\ 3131}} \equiv EW_{\mathrm{BeII\ 3131}} - \delta EW$, from which the Be abundance [A'(Be)] corresponding to the case of using [Fe/H] of the star (as given) was calculated. Finally, the differences between A'(Be) and A(Be) may be regarded as errors of A(Be) caused by uncertainties in the treatment of blending lines. [Here, the dispersion among these differences is essentially important, since the absolute value of the difference itself depends on the error in the gf value of the Fe I 3131.043 line.] The resulting discrepancies of δA(Be) [$\equiv A'$(Be) $- A$(Be)] computed for the program stars are also given in electronic table E3, which revealed that δA(Be) mostly ranges from ~ -0.3 to $+0.1$ (dispersion of $\sim \pm 0.2$ dex) for FGK stars and ~ -0.2 to ~ 0.0 (dispersion of $\sim \pm 0.1$ dex) for solar-analog stars. Accordingly, the corresponding errors may be estimated as being $\sim \pm 0.1$ dex and $\sim \pm 0.2$ dex for solar analogs and FGK stars, respectively.[7] It should be remarked, however, that this discussion is valid only for non-Be-depleted cases. As the strength of the Be line decreases, the error in A(Be) should be enhanced accordingly, since the contribution of the Fe I line would become comparatively more important [actually a considerably large $|\delta A$(Be)$|$ amounting to ~ 1 dex is even seen for a few Be-deficient cases].

3.5.   Comparison with Previous Work

The A(Be)'s resulting from this study and those derived by Santos et al. (2002, 2004a, 2004b) and Boesgaard and Hollek (2009) for stars in common are compared in figure 7. We can see from this figure that Santos et al.'s results (mostly planet-host stars at 6300 K $\gtrsim T_{\mathrm{eff}} \gtrsim$ 5400 K, tending to be metal-rich) are systematically lower than ours by ~ 0.1–0.3 dex, whereas Boesgaard and Hollek's results (for stars at 6200 K $\gtrsim T_{\mathrm{eff}} \gtrsim$ 5800 K) are slightly higher than ours by ~ 0.1–0.2 dex. Regarding the comparison with the latter Boesgaard and Hollek's case, the appreciable discrepancies of ~ 0.2 dex shown by two Be-deficient stars [A(Be) $\lesssim 1$;
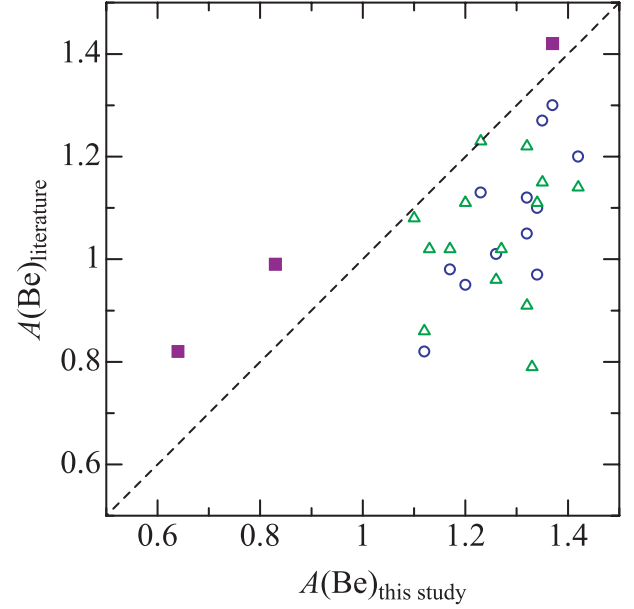

Fig. 7. Comparison of the Be abundances derived in this study with the literature values: filled squares $\cdots$ Boesgaard and Hollek (2009; 3 stars in common); open circles $\cdots$ Santos et al. (2002; 13 stars in common); open triangles $\cdots$ Santos et al. (2004a, 2004b; 14 stars in common).

HD 89125 and HD 142860] may (at least partly) be attributed to the difference in the adopted atmospheric parameters, since the fact that their $T_{\mathrm{eff}}/\log g$ is lower/higher by ~ 50 K/~ 0.1 dex than ours makes their A(Be) comparatively increase by ~ 0.1 dex. On the other hand, in the former case, we do not see any notable systematic differences in the adopted parameters between Santos et al. and ours, which suggests that the discrepancies may presumably stem from some difference in the A(Be) determination procedure.

4.   Discussion

4.1.   General Behavior of Be in FGK Stars

Now that the Be abundances have been determined, we first discuss their general characteristics for the whole combined sample of 205 stars (118 solar analogs and 87 FGK standards).

4.1.1.   Metallicity dependence of Be

The A(Be) values obtained for all stars are plotted against [Fe/H] in figure 8b, where the results for A(Li) (Paper I; Takeda & Kawanomoto 2005) are also shown (figure 8a) for a comparison. It is apparent from these figures that the trends are markedly different between these two cases: while A(Li) are rather uniformly distributed over a considerably large span of $\gtrsim 2$ dex, A(Be) tends to be confined to a narrow region between ~ 1 and ~ 1.5 (except for $T_{\mathrm{eff}} > 6000$ K stars showing deficiencies).

The important problem to be clarified before discussing the possibility of a Be abundance variation is the primordial Be abundance a star would have had when it was born. While it is known that A(Be) and [Fe/H] are well correlated with each other in the metal-poor regime ([Fe/H] $\lesssim -1$), the behavior for near-solar metallicity stars, like the present sample

---

7   In a typical example case of $EW_{\mathrm{BeII\ 3131}} \sim 70$–90 mÅ and $EW_{\mathrm{FeI\ 3131}} \sim$ 30 mÅ for a solar analog, a perturbation of δA(Fe) ~ 0.2 dex leads to $\delta EW_{\mathrm{FeI\ 3131}} \sim 7$ mÅ. This change of $\delta EW \sim 7$ mÅ upon $EW_{\mathrm{BeII\ 3131}}$ (~ 70–90 mÅ), in turn, varies A(Be) by ~ 0.1 dex.
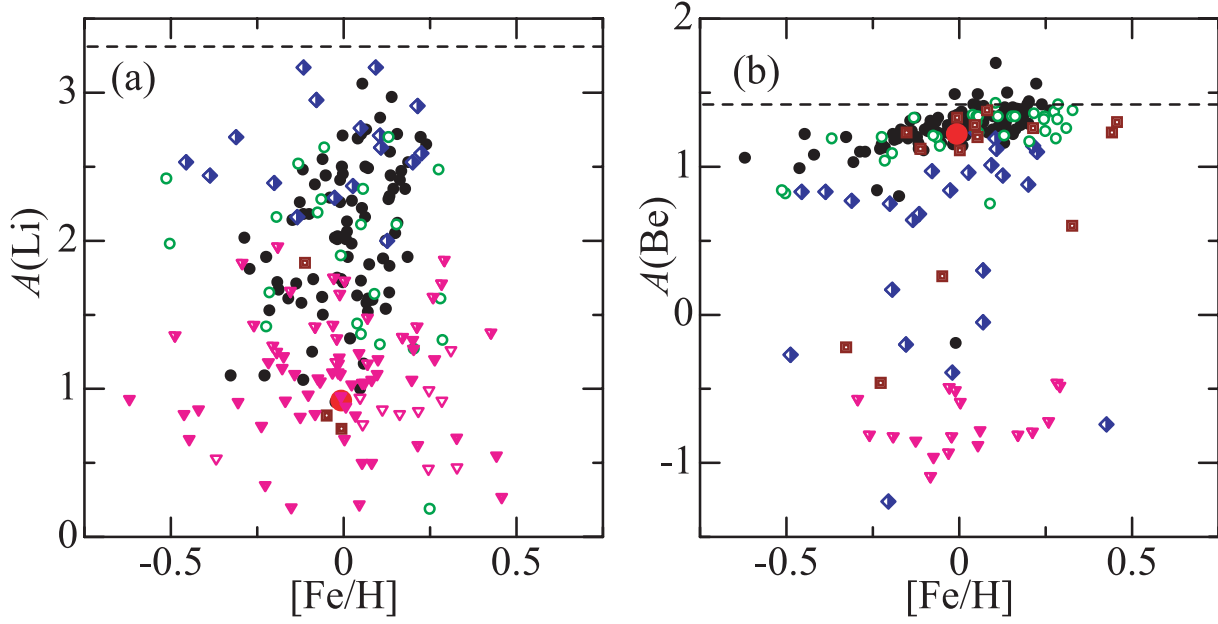
Fig. 8. Li and Be abundances plotted against the metallicity: (a) A(Li) vs. [Fe/H]; (b) A(Be) vs. [Fe/H]. The same meanings of the symbols as described in the caption of figure 2. Note that the (pink) downward triangles indicate the upper limit values. The meteoritic abundances (3.31 for Li, 1.42 for Be; cf. Anders & Grevesse 1989) are indicated by the horizontal dashed lines.

$(-0.5 \lesssim$ [Fe/H] $\lesssim +0.4)$, is still uncertain.

Boesgaard et al.'s (2004a) analysis of solar-type dwarfs suggested δA(Be)$/\delta$[Fe/H] $\simeq 0.38$, whereas Boesgaard and Hollek (2009) recently argued (in their Be abundance study of one solar-mass stars around $T_{\rm eff} \sim 6000$ K) that a steeper slope of δA(Be)$/\delta$[Fe/H] $\simeq 0.86$ holds not only for metal-poor stars, but also for those up to [Fe/H] ~ 0 continuously. Meanwhile, there is a chemical evolution model that predicts a nearly constant (though rather complex) A(Be) at $-1 \lesssim$ [Fe/H] (cf. figure 4 of Casuso & Beckman 1997).

The upper envelope of our A(Be) vs. [Fe/H] relation in figure 8b indicates that A(Be) certainly increases with [Fe/H]. According to the linear-regression analysis applied to solar analogs [mostly with $1.0 \le A$(Be) ≤ 1.5, while excluding several outliers] at $-0.3 \lesssim$ [Fe/H] $\lesssim +0.3$, we obtained A(Be) $= 1.28\,(\pm 0.01) + 0.49\,(\pm 0.05)$ [Fe/H], which suggests δA(Be)$/\delta$[Fe/H] ~ 0.5 (i.e., just the midpoint between 0 and 1). Accordingly, when showing the trend of Be for discussing the possibility of depletion-induced abundance changes, we present two kinds of figures in terms of A(Be) as well as [Be/Fe], considering that the relevant information may be revealed by these two.

4.1.2. Abundance trend with T_{eff}

Figures 9a and b display the distribution of A(Be) and [Be/Fe] against $T_{\rm eff}$, from which we can notice the following characteristics:

— For F-type stars ($T_{\rm eff} > 6000$ K), Be abundances show a considerably large spread amounting to ~ 2 dex, as has been already reported in previous studies (e.g., Boesgaard et al. 2004b).

— Regarding early-G stars at $6000\,{\rm K} > T_{\rm eff} > 5500\,{\rm K}$, the main targets of this study, we can recognize that most stars have similar Be abundances near to the solar value, but there *do* exist

several stars showing conspicuous Be depletion. Interestingly, all of these stars have almost the same $T_{\rm eff}$ as the Sun. Accordingly, we may state that the existence of "Be-gap" (i.e., a marked depression of Be abundances in a narrow $T_{\rm eff}$ range) suggested by Santos et al. (2004a) has been confirmed (in a limited sense) in our solar-analog sample. The origin of Be depletion for these stars is discussed in subsection 4.2.

— Regarding late-G or early-K stars ($5500\,{\rm K} > T_{\rm eff} > 5000\,{\rm K}$), Be is definitely depleted for three lowest $T_{\rm eff}$ stars ($T_{\rm eff} < 5250\,{\rm K}$), which is understandable because they are rather evolved subgiants (cf. figure 2b), and envelope mixing is considered to be enhanced. If we restrict ourselves to dwarfs, there may be a weak signature that depletion gradually begins at $T_{\rm eff} \lesssim 5500$ K.

— We could not confirm the decreasing tendency of A(Be) with a lowering of $T_{\rm eff}$ reported by Santos et al. (2004a, 2004b). Rather, the upper envelope of A(Be) (and especially of [Be/Fe]) appears to slightly increase with a decrease in $T_{\rm eff}$ from $T_{\rm eff} \sim 6500$ K down to $T_{\rm eff} \sim 5500$ K. Actually, this is a tendency already suggested by Boesgaard and Hollek (2009; cf. their figure 9).

4.1.3. Be in planet-host stars

It worth examining whether there is any difference in the behavior of Be between planet-host stars (PHS) and non-planet-host stars (non-PHS), since our sample includes 18 such stars harboring giant planets (5 in the solar analogs and 13 in the FGK standards), the Be abundances of which are summarized in table 2. As can be seen from this table, the A(Be) values for most (sixteen) PHS are around the solar value ($\sim 1.2 \pm 0.2$) to within $\lesssim 0.2$ dex, similar to other solar-type non-PHS, while only two PHS at $T_{\rm eff} \sim 6400$ K show a marked depletion as other F-type non-PHS. Accordingly, we may state that any meaningful difference can not be noticed with regard
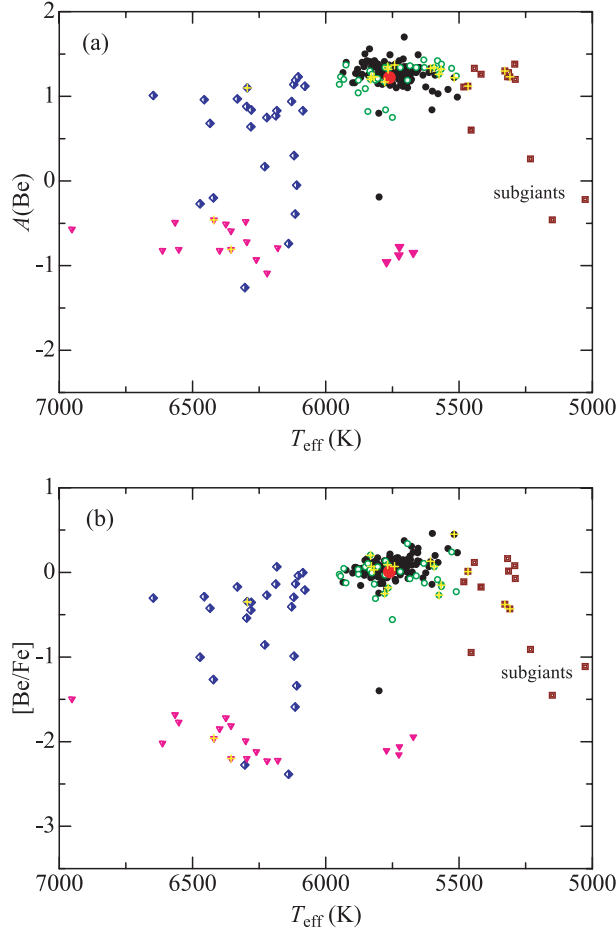
Fig. 9. Be abundances plotted against the effective temperature. (a) A(Be) vs. $T_{\rm eff}$; (b) [Be/Fe] vs. $T_{\rm eff}$. The same meanings of the symbol types as described in the caption of figure 2. The downward triangles (pink) denote the upper-limit values for the indeterminable cases where the Be II 3131.066 line is too weak to be detectable. The planet-host stars are indicated by overplotting yellow crosses.

to the surface Be abundances between two samples of stars with and without giant planets (which can be confirmed by plotting the data of these 18 stars on figure 9). This result is essentially a reconfirmation of the conclusion of Santos et al. (2002, 2004b, 2010). In this connection, it is worth pointing out that HD 186408 [16 Cyg A, non-PHS, A(Be) $= 1.34$, A(Li) $= 1.37$] and HIP 96901 [16 Cyg B, PHS, A(Be) $= 1.37$, A(Li) < 1.06], quite similar Sun-like non-PHS and PHS stars constituting a visual binary system, have practically the same A(Be) despite the distinct difference in A(Li). Recently, Delgado Mena et al. (2011) reported that A(Be) in PHS tends to be lower than that in non-PHS only in the low-$T_{\rm eff}$ region of ~ 5000 K. Although such a tendency could not be confirmed in our results, we can not state much about their claim, since the number of such cool stars in our sample is too small for any meaningful discussion.

4.2. Be Abundances in Solar-Analog Stars

4.2.1. Evidence of rotation-dependence

We now confine ourselves to the main topic of this study: How is the behavior of the Be abundances of 118

solar-analogs? Do they have any correlation with the Li abundances, or other stellar properties, such as rotation or age?

We can see several interesting characteristics in figure 10, where the results of A(Be) and [Be/Fe] are plotted against A(Li), $v_{\rm e} \sin i$, $r_0(8542)$, and $\log age$.

— While most stars have similar Be abundances around the solar value within $\lesssim 0.2$ dex, 4 stars are markedly discrepant from the general trend of A(Be), for which the Be II 3131 line is undetectable, suggesting a drastic Be depletion by more than ~ 2 dex: HIP 17336 [A(Be) < -0.85], HIP 32673 (< -0.78), HIP 64150 (< -0.88), and HIP 75676 (< -0.96).[8] It is important to note that, in all of these Be-depleted stars, (i) Li is also depleted, (ii) $v_{\rm e} \sin i$ is the lowest class, and (iii) $r_0(8542)$ is also the lowest class (that is, these 4 stars are clustered in the lower-left corner in figures 10a–c as well as a′–c′). This indicates that slow rotation must be the key factor (at least one of the causes, even if not the only one) triggering such an exceptionally drastic dearth of Be in solar-analogs.

— Furthermore, regarding the other stars (and the Sun) having apparently similar Be abundances, we can notice from figures 10a–c as well as a′–c′ a weak, but significant, trend that A(Be) (and also [Be/Fe], though less clearly) shows a gradual rise with increasing A(Li), $v_{\rm e} \sin i$, and $r_0(8542)$. This may be interpreted that some kind of very gradual Be depletion mechanism takes place even in these "superficially normal Be stars," acting more efficiently as stellar rotation becomes slower.

4.2.2. What are Be-depletion mechanisms like?

Considering these two facts, we may conclude that stellar rotation plays a significant role in controlling the surface Be abundances of solar-analog stars. However, it is rather hard to imagine that both the drastic Be depletion for a tiny fraction of stars and the more gradual alteration for the majority of stars can be attributed to the same physical process. Accordingly, we would propose that two kinds of Be-depletion mechanism may operate in the envelope of Sun-like stars; i.e., the "strong" and "weak" ones:

— The "strong" process should work only in limited cases where special conditions are satisfied; but once it has been triggered, surface Be is depleted very efficiently. At least, very slow rotation (and presumably also the near-solar $T_{\rm eff}$) may be counted as the necessary (if not sufficient) condition for this process to work, though we have no specific idea which kind of physical process it is.[9]

— On the other hand, the "weak" process is relevant for

---

[8] HIP 88945 with A(Be) $= -0.19$ should also be classified as a Be-depleted star. However, as already remarked in Paper II, this star has rather unusually high $v_{\rm e} \sin i$ and $r_0(8542)$ in spite of its low A(Li), which means that it does not follow the general trend of A(Li)–$v_{\rm e} \sin i$–$r_0(8542)$ relation established in Paper II. Therefore, we should be cautious in interpreting the results for this outlier star.

[9] An anonymous referee kindly suggested a possibility that these four conspicuously Be-deficient stars might belong to a group of stars having rotated very rapidly in the past (and suffered substantial Be depletion due to rotation-induced mixing) but considerably spun down at present, as suggested from the modeling of ultra-Li-deficient halo stars (Pinsonneault et al. 1999, 2002), which is an intriguing hypothesis. However, we should bear in mind that these 4 stars have parameters quite similar to the Sun (actually, 3 are the solar twin candidates sorted out in table A.1 of Paper I), also with respect to $v_{\rm e} \sin i$. So, if this is really the case, we should regard that the rotational braking of these stars must have been so strong that any trace of having being a rapid rotator in the past has completely disappeared.
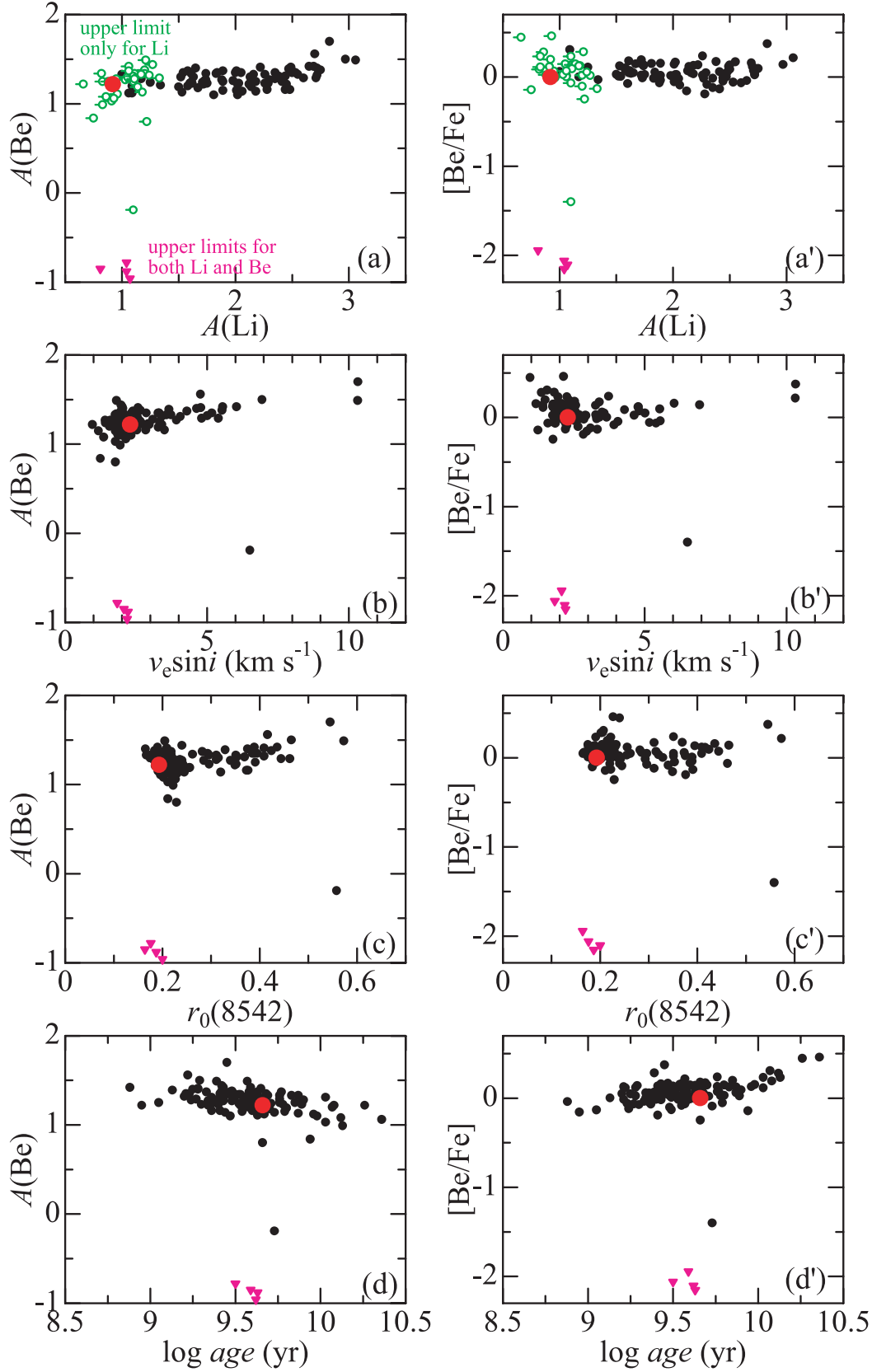
Fig. 10. Be abundances of 118 solar analogs (and the Sun) plotted against the Li abundance (from Paper I; panels a/a′), the projected rotational velocity (from Paper II; panels b/b′), the residual flux at the Ca II 8542 line center (from Paper II; panels c/c′), and the age (from Paper I; panels d/d′). The left panels are for A(Be), while the right ones are for [Be/Fe]. Pink downward triangles indicate the upper-limit values for both Be and Li abundances (four stars). Regarding the green open circles (with leftward ticks) in panels (a) and (a′), the upper-limit values are relevant only for the Li abundances.

Table 2. Be abundances of 18 planet-host stars.

Star	$T_{\rm eff}$ (K)	$\log g$ (cm s^{-2})	[Fe/H] (dex)	A(Be) (dex)	[Be/Fe] (dex)	A(Li) (dex)	Remark
HIP 26381	5518	4.47	−0.45	1.22	+0.45	($<$0.66)	solar analog
HIP 53721	5819	4.19	−0.02	1.23	+0.03	1.75	solar analog
HIP 59610	5829	4.34	−0.06	1.23	+0.07	1.62	solar analog
HIP 90004	5607	4.42	−0.02	1.33	+0.13	($<$1.17)	solar analog
HIP 96901	5742	4.32	+0.08	1.37	+0.07	($<$1.06)	solar analog
HD 120136	6420	4.21	+0.28	($<$−0.46)	($<$−1.96)	($<$1.71)	standard ($T_{\rm eff} > 6000$)
HD 169830	6355	4.14	+0.17	($<$−0.81)	($<$−2.20)	($<$1.35)	standard ($T_{\rm eff} > 6000$)
HD 179949	6294	4.49	+0.23	1.10	−0.35	2.59	standard ($T_{\rm eff} > 6000$)
HD 143761	5832	4.25	−0.22	1.20	+0.20	1.42	standard ($6000 > T_{\rm eff} > 5500$)
HD 217014	5779	4.30	+0.20	1.17	−0.25	1.27	standard ($6000 > T_{\rm eff} > 5500$)
HD 195019	5768	4.11	+0.04	1.35	+0.09	1.44	standard ($6000 > T_{\rm eff} > 5500$)
HD 134987	5766	4.37	+0.28	1.32	−0.18	($<$0.92)	standard ($6000 > T_{\rm eff} > 5500$)
HD 168443	5593	4.16	+0.06	1.34	+0.06	($<$0.76)	standard ($6000 > T_{\rm eff} > 5500$)
HD 217107	5575	4.18	+0.31	1.26	−0.27	($<$1.26)	standard ($6000 > T_{\rm eff} > 5500$)
HD 210277	5567	4.44	+0.25	1.32	−0.15	($<$0.46)	standard ($6000 > T_{\rm eff} > 5500$)
HD 117176	5466	3.80	−0.11	1.12	+0.01	1.85	standard ($5500 > T_{\rm eff}$)
HD 75732	5328	4.58	+0.46	1.30	−0.38	($<$0.27)	standard ($5500 > T_{\rm eff}$)
HD 145675	5309	4.45	+0.44	1.23	−0.43	($<$0.55)	standard ($5500 > T_{\rm eff}$)

* The data of atmospheric parameters and Li abundances were taken from Paper I (for solar analog stars) as well as Takeda et al. (2005) and Takeda and Kawanomoto (2005) (for standard stars). See electronic tables E1 and E2 for more detailed information concerning these stars as well as for the complete data for the whole 205 stars.

most stars, steadily and slowly acting to reduce Be in the outer envelope, which should be more efficient as the rotation becomes slower. Such a mechanism is likely to be the bit-by-bit destruction of Be nuclei at the bottom of the convection zone (where the Be burning temperature of $\sim 3.5 \times 10^6$ K is not yet reached; cf. figure 1) by an appropriate mixing of the boundary layer caused by differential rotation-induced shear, such as that considered by Bouvier (2008) (cf. subsection 1.2), since this theory most reasonably explains the observational fact among several possible A(Be)-changing mechanisms investigated so far.[10]

— In cases where such a long-lasting "weak" depletion mechanism takes place, it is expected that older stars show a larger Be-deficiency. Unfortunately, we can not make a decisive answer about this test, since A(Fe) and [Be/Fe] exhibit different behaviors due to the tight [Fe/H] vs. *age* relation (figure 2c); i.e., while A(Be) certainly shows this expected trend (figure 10d), the tendency of [Be/Fe] is just the opposite (figure 10d′). In this connection, we should also pay attention to the possibility that mixing may be rather suppressed in old stars, because they are generally of low metallicity, which makes convection less active.

4.2.3. *Is solar Be abundance primordial?*

The consequence from figure 10, that any solar-analog stars must have (more or less) suffered Be-depletion in the envelope with its extent depending on the rotational velocity, naturally implies that most stars (especially slowly rotating ones) currently have surface Be abundances appreciably lower than the primordial values they had at their birth. Then, since our Sun definitely belongs to the slow-rotation group ($v_{\rm e} \sin i \sim 2$ km s^{-1}), a significant discrepancy between the current and the initial Be abundances is expected. We may estimate this amount as ~ 0.2–0.3 dex from the abundance difference between $v_{\rm e} \sin i \sim 2$ km s^{-1} and $v_{\rm e} \sin i \sim 10$ km s^{-1} in figures 10b or 10b′, assuming that the depletion is sufficiently small for the latter high-rotation case. Interestingly, this value quite reasonably explains the observed difference between the current photospheric Be abundance (1.22: from this study) and the meteoritic Be abundance (1.42: Anders & Grevesse 1989). As a matter of fact, this meteoritic–photospheric discordance of Be was previously regarded as being due to a mixing-induced depletion in the solar envelope.

However, Balachandran and Bell (1998) argued against this scenario, insisting that this discrepancy simply stemmed from an erroneous underestimation of the solar Be abundance due to an imperfect treatment of the UV continuum opacity (so-called "missing opacity") at the Be II line region. They showed that a photospheric abundance consistent with the meteoritic value is obtained by increasing the continuum opacity by a factor of 1.6. Based on this argument, they concluded that the mixing in the solar envelope is too shallow to affect the Be abundance at the surface, in which the primordial (meteoritic) abundance of A(Be) ~ 1.4 is retained unchanged. Furthermore, Asplund (2004) corroborated their conclusion based on a discussion of O abundance matching between different lines, though it may not be regarded as direct evidence for the existence of missing opacity.

---

[10] For example, Deliyannis and Pinsonneault (1997) theoretically studied the effect of mass loss, diffusion, and wave-driven as well as rotational mixing in the envelope of late F stars. Similarly, Charbonnel and Lagarde (2010) recently examined the role of rotation-induced mixing along with the thermohaline instability for the Li depletion in the envelope of 1–4 $M_\odot$ stars. However, the conclusions of these studies suggest that faster rotation enhances the mixing, which is just the opposite to what we found here.
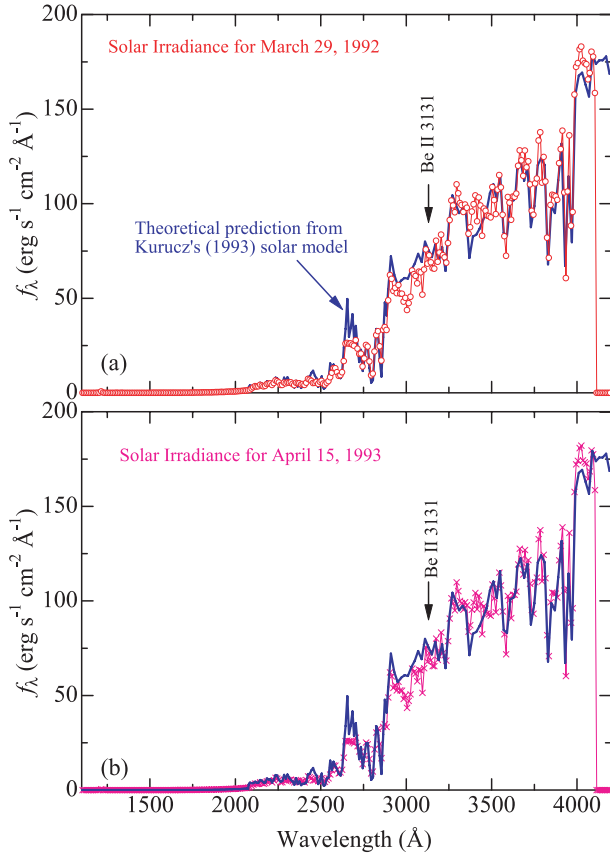
Fig. 11. Comparison of the absolute solar flux at the position of the Earth in the 1100–4100 Å region. Theoretical fluxes computed with Kurucz's (1993) ATLAS9 solar model atmosphere (reduced to the values at the Earth) are depicted by thick lines, while the observed data of Woods et al. (1996) on two different dates are shown by line–connected symbols. (a) Experiment on 1992 March 29 (open circles); (b) Experiment on 1993 April 15 (crosses).

Yet, Balachandran and Bell's (1998) argument conflicts with our interpretation mentioned above. Therefore, we decided to examine by ourselves as to whether such a UV missing opacity problem really exists around the Be II 3131 line region. The comparison of the observed solar flux energy distribution at the Earth (i.e., just outside of Earth's atmosphere) taken from Woods et al. (1996) with the theoretical flux computed from Kurucz's (1993) ATLAS9 solar model atmosphere (reduced to the value at the Earth[11]) is shown in figure 11. Rather unexpectedly, as can be seen from this figure, we could not confirm any such significant flux discrepancy between theory and observation at $\lambda \sim 3131$ Å that may suggest the existence of missing opacity in the model.

This result casts doubt about the reliability of the conclusion made by Balachandran and Bell (1998), in which we actually notice some questionable points:
— They appear to put too much weight on the delicate difference seen in the profiles of the spectral line at the $\lambda \sim 3128$ Å and $\lambda \sim 3131$ Å region in order to justify their claim,

stating that adding an extra amount of UV opacity significantly improves the fit between the theoretical and observed line shapes. In our opinion, however, the solution to such a line-profile problem may be found in some other ways, such as adjusting the line-broadening function due to macroturbulence (known to be depth-dependent in the solar atmosphere).
— If confirming the existence of missing opacity is the central issue, the modeled absolute flux distribution should be compared with the observed solar ultraviolet irradiance, as done in figure 11. We would point out, however, that any direct evidence of discrepancy between theoretical and observational solar fluxes just at $\lambda \sim 3131$ Å has never been presented, as far as we see the papers by Gustafsson and Bell (1979) or Bell, Paltoglou, and Trippico (1994), which Balachandran and Bell (1998) quoted for the indication of too large calculated solar flux.

Of course, it is premature to conclude that their consequence is incorrect based on this argument alone; further checks or reconfirmation may be required.[12] Yet, at any event, given that the observed solar UV flux is well reproduced by the ATLAS9 model, which we also invoked for Be abundance determinations, there is no reason for us to be concerned about any missing opacity. We may thus regard that $A_\odot(\text{Be}) = 1.22$ derived in this study represent the "real" Be abundance in the solar photosphere, and that its being lower by 0.2 dex compared to the meteoritic abundance can be attributed to the result of a mild depletion in the solar envelope. In short, the currently observed Be abundance in the photosphere of the Sun (and in solar-analog stars) should not be regarded as representing the primordial abundance, which must have gradually varied during the lifetime so far.

5. Conclusion

We conducted an extensive Be abundance analysis for 118 solar analogs (along with 87 FGK standard stars) in order to clarify the controversial issue of how the Be abundances for Sun-like stars behave themselves at $6000\,\text{K} \gtrsim T_{\text{eff}} \gtrsim 5500\,\text{K}$ in connection with the Li abundance and stellar parameters, such as rotation, age, and activity index. In particular, we wanted to answer the question "Do $A(\text{Be})$'s show any sign of depletion like $A(\text{Li})$? Or, alternatively, are they almost constant at the primordial Be abundances being unchanged?"

The observed spectra of 205 targets in the near-UV region including Be II resonance lines were obtained in the 2009–2010 season by using the High-Dispersion Spectrograph of the Subaru Telescope. The Be abundance of each star was determined by applying the spectrum synthesis technique (coupled with the automatic best-fit solution finding algorithm) to the 3130.65–3131.35 Å region, comprising the Be II line at 3131.066 Å.

Inspecting the trend of the Be abundances for the whole sample, we found that $A(\text{Be})$'s for a majority of stars (especially for the solar-type) are confined around the solar value,

---

[11] $f_\lambda^{\text{th}} \equiv 4\pi H_\lambda^{\text{th}}(0)\,(R/d)^2$, where $H_\lambda^{\text{th}}(0)\,[\equiv (1/2)\int_0^1 \mu I_\lambda^{\text{th}}(0,\mu)d\mu]$ is the Eddington flux at the surface of the Sun, R is the solar radius, and d is the Sun–earth distance.

[12] In this connection, Smiljanic et al. (2009) reported that an increase in the Fe I bound-free opacity by a factor of 1.6 (the enhancement factor proposed by Balachandran and Bell) in a test model with [Fe/H] $= -0.5$ hardly affects the resulting Be abundance in the practical sense (i.e, only 0.022 dex), suggesting that UV missing opacity is insignificant.

Table 3. Non-LTE effect on Be abundance determination from the Be II 3131.066 line.

Model	T_{eff} (K)	$\log g$ (cm s^{-2})	[Fe/H] (dex)	v_t (km s^{-1})	A_{input} (dex)	(EW^L) (mÅ)	EW_0^N (mÅ)	EW_{-3}^N (mÅ)	Δ_0^N (dex)	Δ_{-3}^N (dex)
T50G40P00	5000	4.0	0.00	1.5	1.15	(62.5)	62.2	60.5	+0.01	+0.03
T55G40P00	5500	4.0	0.00	1.5	1.15	(80.0)	80.0	78.9	0.00	+0.01
T60G40P00	6000	4.0	0.00	1.5	1.15	(89.7)	88.3	87.7	+0.02	+0.03
T65G40P00	6500	4.0	0.00	1.5	1.15	(85.5)	79.4	79.1	+0.09	+0.09

* The first five columns give the atmospheric parameters of each model. A_{input} in column 6 is the input (solar) Be abundance (Anders & Grevesse 1989), with which three kinds of equivalent widths [LTE, non-LTE ($\log k = 0$), and non-LTE ($\log k = -3$); k is the reduction factor of classical H I collision rates] are computed as presented in columns 7–9. Columns 10 and 11 give the non-LTE corrections for each case of k. Δ_0^N is defined as $A_0^N - A_0^L$, where A_0^N and A_0^L are the non-LTE ($k = 1$) and LTE abundances inversely derived from EW_0^N, respectively. [Note that A_0^N is essentially equal to A_{input}.] Regarding Δ_{-3}^N, a similar definition applies.

though stars showing conspicuous Be depletion do exist (especially for F-type stars at $T_{eff} \gtrsim 6000$ K). This makes a marked contrast to the case of A(Li), which tends to show a rather uniform spread with a considerably large dispersion of $\gtrsim 2$ dex. The upper envelope of the A(Be) vs. [Fe/H] relation suggests that A(Be) increases with [Fe/H] with a slope of $\delta A(Be)/\delta[Fe/H] \sim 0.5$ in the metallicity range of $-0.5 \lesssim [Fe/H] \lesssim +0.4$. We could not find any difference in Be between stars with and without planets.

Regarding the Sun-like stars, while most of them are superficially similar in terms of their A(Be) at $\sim 1.2 \pm 0.2$, 4 out of 118 stars turned out to be strikingly Be-deficient (by $\gtrsim 2$ dex); these 4 stars have the lowest $v_e \sin i$, the lowest stellar activity, and considerably depleted A(Li). Moreover, even for the other majority showing an apparent similarity in Be, we can recognize a tendency that A(Be) gradually increases with an increase in $v_e \sin i$, A(Li), and $r_0(8542)$.

These results suggest that any solar-analog star (including the Sun) generally suffers some kind of rotation-dependent Be depletion, for which we suspect two kinds of mechanisms may operate. The "strong" process should work only in limited cases under special conditions, but depletes surface Be very efficiently once triggered, whereas the "weak" process acts on most stars and slowly reduce Be in the outer envelope. The contributions of theoreticians are desirably awaited toward developing a reasonable model/theory accounting for the observational facts.

According to our findings, the occasionally stated view "Be-depletion is irrelevant to G-type dwarfs with $T_{eff} \lesssim 6000$ K, which have similar Be abundances and retain their original composition" is not correct; the Be abundances of such stars are generally considered to have more or less suffered reduction compared to the primordial values. The difference of ~ 0.2 dex between the current solar photospheric Be abundance and the meteoritic Be abundance may be interpreted in this way. This means that we do not lend support for the widely mentioned scenario of "erroneous underestimation of Be abundances due to the neglect of UV missing opacity."

This research has made use of the SIMBAD database, operated by CDS, Strasbourg, France.

Appendix. Non-LTE Effect on the Be II 3131 Line
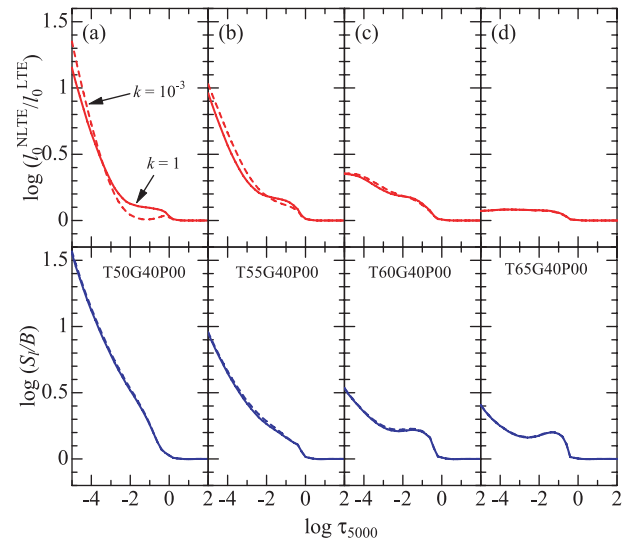
The non-LTE effect on the formation of Be II 3130–3131

Fig. 12. Departure from LTE for the Be II $2s\ ^2S$–$2p\ ^2P°$ transition (multiplet 1) corresponding to the Be II lines at 3130.421 Å and 3131.066 Å, computed for four representative atmospheric models with different T_{eff} but with the same $\log g$ (4.0) and the metallicity (solar). The upper and lower panels show the depth-dependence of the NLTE-to-LTE line-center opacity ratio and the ratio of the line source function to the Planck function, respectively. Panels (a), (b), (c), and (d) correspond to T_{eff} of 5000 K, 5500 K, 6000 K, and 6500 K, respectively. Solid lines ··· results for $k = 1$ (classical treatment of the H I collision without any correction); dashed lines ··· results for $k = 10^{-3}$ (reduction of the classical H I collision rates by a factor of 10^{-3}; i.e., practically to a negligible level).

doublet has already been studied by several investigators (see, Asplund 2005 for a review of the previous work), such as Chmielewski, Müller and Brault (1975) (for the Sun), Shipman and Auer (1979) (for the Sun), Kiselman and Carlsson (1995) (for the Sun, Procyon, and HD 140283), and García López, Severino, and Gomez (1995a) (for the Sun and metal-poor stars). All of these performed non-LTE calculations on the Be I + Be II atomic model, and arrived at almost the same conclusion, that the non-LTE correction for deriving the Be abundance from the Be II 3130–3131 resonance lines is insignificant.

Since FGK stars covering a rather wide T_{eff} range (7000 K $\gtrsim T_{eff} \gtrsim 5000$ K) are of concern in the present study, and we are interested in how the treatment of neutral-hydrogen

collisions influences the results (which has not been considered in previous studies of Be line formation), we carried out some test calculations.

Our atomic model of Be comprises 20/22 terms and 28/89 radiative transitions for Be I/Be II, including up to Be I $2s\,6p\;{}^1$P (71746 cm^{-1} from the ground level) and Be II $7g\;{}^2$G (137925 cm^{-1} from the ground level), which was constructed from the atomic-line database compiled by Kurucz and Bell (1995). The data from TOPbase (Cunto & Mendoza 1992) were adopted for the photoionization cross sections for the lowest 9 and 8 terms of Be I and Be II, respectively. As for other computational details (e.g., electron-collision rates, photoionization rates for the remaining terms, collisional ionization rates, treatment of collisions with neutral-hydrogen atoms, etc.), we followed the recipe described in sub-subsection 3.1.3 of Takeda (1991).

Statistical-equilibrium calculations were carried out for four models with $T_{\rm eff} = 5000$, 5500, 6000, and 6500 K (each with the same solar-metallicity and $\log g = 4$). Regarding the treatment of neutral-hydrogen collision rates, we tested two cases: (i) classical H I rates are used uncorrected ($k = 1$), (ii) classical H I rates are drastically reduced by multiplying them by a factor of $k = 10^{-3}$.

In figure 12 are shown the $S_{\rm L}(\tau)/B(\tau)$ (the ratio of the line source function to the Planck function, and nearly equal to $\simeq b_{\rm u}/b_{\rm l}$, where $b_{\rm l}$ and $b_{\rm u}$ are the non-LTE departure coefficients for the lower and upper levels, respectively)

and $l_0^{\rm NLTE}(\tau)/l_0^{\rm LTE}(\tau)$ (the NLTE-to-LTE line-center opacity ratio, and nearly equal to $\simeq b_{\rm l}$) for the multiplet 1 transition ($2s\;{}^2$S–$2p\;{}^2$P°) relevant to the Be II 3130–3131 doublet lines. Also, the LTE and non-LTE equivalent width for the Be II 3131.066 line and the corresponding non-LTE abundance correction were computed for each case, which are summarized in table 3.

Inspecting figure 12 and table 3, we can make the following conclusions regarding the non-LTE effect on the Be II 3131.066 line:

— While an appreciable departure from LTE is noticed in the line opacity (increased opacity acting to strengthen absorption) as well as in the line source function (enhanced source function acting to dilute/weaken absorption), the net effect on the equivalent width is quite small, because both act in the opposite direction (see, e.g., Asplund 2005 or García López et al. 1995a for more details concerning the line-formation mechanism).

— The results are practically independent of how the H I collision is treated, which reflects that the formation of this UV transition is controlled by (not collisional but) radiative processes.

— We can neglect the non-LTE abundance correction (especially for solar-type stars with $T_{\rm eff} \lesssim 6000$ K), since its extent is on the order of a few hundreds dex at most, though it may become noticeable for F-type stars of $T_{\rm eff} \gtrsim 6500$ K at a level of ~ 0.1 dex (positive correction).

References

Anders, E., & Grevesse, N. 1989, Geochim. Cosmochim. Acta, 53, 197

Asplund, M. 2004, A&A, 417, 769

Asplund, M. 2005, ARA&A, 43, 481

Balachandran, S. C., & Bell, R. A. 1998, Nature, 392, 791

Baumann, P., Ramírez, I., Meléndez, J., Asplund, M., & Lind, K. 2010, A&A, 519, A87

Bell, R. A., Paltoglou, G., & Tripicco, M. J. 1994, MNRAS, 268, 771

Boesgaard, A. M., Armengaud, E., King, J. R., Deliyannis, C. P., & Stephens, A. 2004b, ApJ, 613, 1202

Boesgaard, A. M., & Hollek, J. K. 2009, ApJ, 691, 1412

Boesgaard, A. M., McGrath, E. J., Lambert, D. L., & Cunha, K. 2004a, ApJ, 606, 306

Bouvier, J. 2008, A&A, 489, L53

Casuso, E., & Beckman, J. E. 1997, ApJ, 475, 155

Charbonnel, C., & Lagarde, N. 2010, A&A, 522, A10

Chmielewski, Y., Müller, E. A., & Brault, J. W. 1975, A&A, 42, 37

Cunto, W., & Mendoza, C. 1992, Rev. Mex. Astron. Astrofis., 23, 107

Delgado Mena, E., Israelian, G., González Hernández, J. I., Santos, N. C., & Rebolo, R. 2011, ApJ, 728, 148

Deliyannis, C. P., & Pinsonneault, M. H. 1997, ApJ, 488, 836

García López, R. J., Rebolo, R., & Pérez de Taoro, M. R. 1995b, A&A, 302, 184

García López, R. J., Severino, G., & Gomez, M. T. 1995a, A&A, 297, 787

Girardi, L., Bressan, A., Bertelli, G., & Chiosi, C. 2000, A&AS, 141, 371

Gustafsson, B., & Bell, R. A. 1979, A&A, 74, 313

Israelian, G., et al. 2009, Nature, 462, 189

King, J. R., Deliyannis, C. P., & Boesgaard, A. M. 1997, ApJ, 478, 778

Kiselman, D., & Carlsson, M. 1995, in The Light Element Abundances, ed. P. Crane (Berlin: Springer-Verlag), 372

Kurucz, R. L. 1993, Kurucz CD-ROM, No. 13, ATLAS9 Stellar Atmosphere Programs and 2 km/s Grid (Cambridge, MA: Harvard-Smithsonian Center for Astrophysics)

Kurucz, R. L., & Bell, B. 1995, Kurucz CD-ROM, No. 23, Atomic Line Data, (Cambridge, MA: Harvard-Smithsonian Center for Astrophysics)

Kurucz, R. L., Furenlid, I., Brault, J., & Testerman, L. 1984, Solar Flux Atlas from 296 to 1300 nm (Sunspot, New Mexico: National Solar Observatory)

Noguchi, K., et al. 2002, PASJ, 54, 855

Pinsonneault, M. H. 2010, in IAU Symp. 268, Light Elements in the Universe, ed. C. Charbonnel et al. (Cambridge: Cambridge University Press), 375

Pinsonneault, M. H., Steigman, G., Walker, T. P., & Narayanan, V. K. 2002, ApJ, 574, 398

Pinsonneault, M. H., Walker, T. P., Steigman, G., & Narayanan, V. K. 1999, ApJ, 527, 180

Primas, F., Duncan, D. K., Pinsonneault, M. H., Deliyannis, C. P., & Thorburn, J. A. 1997, ApJ, 480, 784

Randich, S. 2010, in IAU Symp. 268, Light Elements in the Universe, ed. C. Charbonnel et al. (Cambridge: Cambridge University Press), 275

Santos, N. C., et al. 2010, in IAU Symp. 268, Light Elements in the Universe, ed. C. Charbonnel et al. (Cambridge: Cambridge University Press), 291

Santos, N. C., García López, R. J., Israelian, G., Mayor, M., Rebolo, R., García-Gil, A., Pérez de Taoro, M. R., & Randich, S. 2002, A&A, 386, 1028

Santos, N. C., Israelian, G., García López, R. J., Mayor, M., Rebolo, R., Randich, S., Ecuvillon, A., & Domínguez Cerdeña, C. 2004b, A&A, 427, 1085

Santos, N. C., Israelian, G., Randich, S., García López, R. J., & Rebolo, R. 2004a, A&A, 425, 1013

Shipman, H. L., & Auer, L. H. 1979, AJ, 84, 1756

Smiljanic, R., Pasquini, L., Bonifacio, P., Galli, D., Gratton, R. G., Randich, S., & Wolff, B. 2009, A&A, 499, 103

Stephens, A., Boesgaard, A. M., King, J. R., & Deliyannis, C. P. 1997, ApJ, 491, 339

Stix, M. 2002, in The Sun, 2nd ed. (Berlin: Springer-Verlag), chap. 6

Takeda, Y. 1991, A&A, 242, 455

Takeda, Y. 1995, PASJ, 47, 287

Takeda, Y. 2007, PASJ, 59, 335

Takeda, Y., Honda, S., Kawanomoto, S., Ando, H., & Sakurai, T. 2010, A&A, 515, A93   (Paper II)

Takeda, Y., & Kawanomoto, S. 2005, PASJ, 57, 45

Takeda, Y., Kawanomoto, S., Honda, S., Ando, H., & Sakurai, T. 2007, A&A, 468, 663   (Paper I)

Takeda, Y., Ohkubo, M., & Sadakane, K. 2002, PASJ, 54, 451

Takeda, Y., Ohkubo, M., Sato, B., Kambe, E., & Sadakane, K. 2005, PASJ, 57, 27 (erratum: 57, 415)

Takeda, Y., & Tajitsu, A. 2009, PASJ, 61, 471

Woods, T. N., et al. 1996, J. Geophys. Res., 101, 9541